

## Haggertyite, a new magnetoplumbite-type titanate mineral from the Prairie Creek (Arkansas) lamproite

IAN E. GREY,<sup>1,\*</sup> DANIELLE VELDE,<sup>2</sup> AND ALAN J. CRIDDLE<sup>3</sup>

<sup>1</sup>CSIRO Division of Minerals, Box 312, Clayton South, Victoria 3169, Australia

<sup>2</sup>Laboratoire de Petrologie Mineralogique, Universite P. & M. Curie, ESA 7058 CNRS, 4 Place Jussieu, 75252-Paris Cedex 05, France

<sup>3</sup>The Natural History Museum, Cromwell Road, London, SW7 5BD

### ABSTRACT

We describe a new titanate mineral, haggertyite, from the Prairie Creek lamproite, Arkansas, U.S.A. The mineral was found exclusively within the reaction zones surrounding small mafic xenoliths in the lamproite. Haggertyite occurs as isolated platelets, typically 30–70  $\mu\text{m}$  maximum dimension, which often show hexagonal morphology. Associated minerals are diopside, olivine, phlogopite, Ti-K-richterite, chrome spinel, ilmenite, priderite, and jeppeite. Haggertyite has a magnetoplumbite-type structure. Typical microprobe analyses give (as wt% oxides)  $\text{TiO}_2 = 36.5\text{--}41.6$ ,  $\text{FeO} = 39.4\text{--}42.9$ ,  $\text{MgO} = 0.7\text{--}3.6$ ,  $\text{BaO} = 9.5\text{--}10.5$ ,  $\text{K}_2\text{O} = 1.3\text{--}1.5$ ,  $\text{Cr}_2\text{O}_3 = 0.0\text{--}5.6$ ,  $\text{MnO} = 0.6\text{--}1.1$ , and  $\text{NiO} = 0.1\text{--}0.4$ . The average composition (based on 19 O atoms and an  $\text{Fe}^{2+}/\text{Fe}^{3+}$  ratio to give 12 small cations) is  $\text{Ba}_{0.68}\text{K}_{0.31}\text{Ti}_{5.05}\text{Fe}_{3.91}^{2+}\text{Fe}_{2.01}^{3+}\text{Mg}_{0.69}(\text{Cr,Mn,Ni})_{0.34}\text{O}_{19}$ . Haggertyite is hexagonal, space group  $P6_3/mmc$ ,  $Z = 2$ ,  $a = 5.9369(1)$ ,  $c = 23.3445(6)$  Å, calculated density of 4.74 g/cm<sup>3</sup>. The structure was refined to  $R_1 = 0.034$  for 339 unique reflections with  $F_o > 4\sigma_{F_o}$ , using single-crystal data. Strongest reflections are [ $d_{\text{calc}}$  (Å),  $I_{\text{calc}}$ ,  $hkl$ ] 2.641 100% (114), 2.795 90% (017), 1.634 47% (02,11), 2.437 46% (023), and 2.963 44% (110). In reflected light, haggertyite is pale gray, opaque, and without internal reflections. It is not discernably pleochroic or birefractant, but it is weakly anisotropic in shades of dark brown. Quantitative specular reflectance measurements for  $R_o$  and  $R_e'$  in air and in oil immersion, respectively, are: 470 nm, 17.3, 16.9, and 5.37, 5.13%; for 546 nm 16.8, 16.35, and 5.19, 4.90%; for 589 nm 16.9, 16.3, and 5.29, 4.92%; and for 650 nm 17.1, 16.4, and 5.42, 5.00%.  $\text{VHN}_{50} = 500$ , with a range of five indentations = 460–540. The mineral is named for Stephen E. Haggerty in honor of his contributions to the mineralogy and crystal chemistry of upper-mantle titanate minerals.

### INTRODUCTION

The Prairie Creek lamproite in Arkansas, U.S.A., has been mined for diamonds and thus is likely to be an important provenance for minerals that provide information on metasomatic reactions in the upper mantle (Mitchell 1985). Titanates are important minerals in this regard because Ti is considered to be introduced metasomatically from deeper regions of the upper mantle along with elements such as Ba and K, and these may react with chromian spinels and other residual minerals to form complex titanates that reflect prevailing  $P$ - $T$ - $X$  (pressure/temperature/composition) conditions (Haggerty et al. 1986).

The new mineral described here was identified in thin sections during the course of a study of minerals from the Prairie Creek lamproite. Electron microprobe analyses on the mineral showed that it was a Ba-Fe titanate containing minor amounts of Mg and K and having a  $[\text{Ba}+\text{K}]/[\text{M}]$  ratio

( $M$  = small cations) similar to that in the magnetoplumbite-type minerals, yimengite,  $\text{K}[\text{Ti}_3\text{Cr}_3\text{Fe}_2\text{Mg}_2]\text{O}_{19}$ , (Dong et al. 1983) and hawthorneite,  $\text{Ba}[\text{Ti}_3\text{Cr}_4\text{Fe}_4\text{Mg}]\text{O}_{19}$ , (Haggerty et al. 1989). It differs from the latter two chromium-rich minerals in that it contains only about 1 wt%  $\text{Cr}_2\text{O}_3$ . A single-crystal structure determination was carried out, which confirmed that the mineral has a magnetoplumbite-type (Adel-skold 1938) structure.

Haggertyite is named for Stephen E. Haggerty, Department of Geology, University of Massachusetts, in recognition of his important contributions to the understanding of the mineralogy and crystal chemistry of titanate minerals from the Earth's mantle. The mineral and the name haggertyite have been approved by the International Mineralogical Association, Commission on New Minerals and New Mineral Names. Type material is deposited at The Natural History Museum, London, as BM 1997,14, at the University of Massachusetts, Department of Geology (Amherst), and at the Smithsonian Institution, Washington, D.C.

\* E-mail: iang@minerals.csiro.au

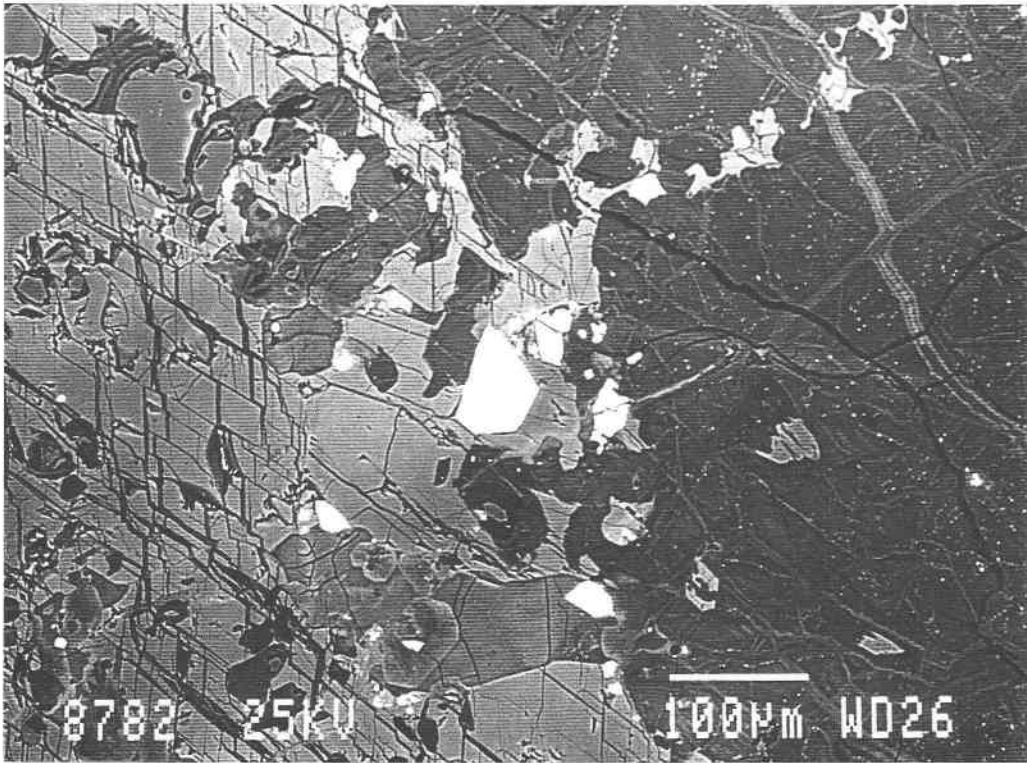


FIGURE 1. Backscattered electron photomicrograph showing a hexagonal haggertyite crystal (white) in contact with richterite (light gray) and serpentized olivine (dark gray). The small light colored crystals are chrome spinels and smaller haggertyite grains.

### OCCURRENCE

Haggertyite was found in several specimens from the Prairie Creek lamproite, previously described as a hypabyssal mica peridotite, collected within the boundaries of the Crater of Diamonds State Park, Arkansas, U.S.A. The outcrop is located near the town of Murfreesboro in Pike County. The geology of the area and the petrology of the rocks present have been described by Mullen and Murphy (1985). A feature of the lamproite is the common occurrence of small (<2 cm) rounded mafic xenolithic rocks. The xenoliths are surrounded by thin (2–3 mm), zoned reaction rims composed mainly of Ti-K richterite, diopside, and phlogopite. The reaction zones are characterized by the absence of perovskite, which is a common accessory mineral in the lamproite. Haggertyite occurs as isolated crystals or in small groups within the reaction zones. The associated minerals are Ti-K richterite, diopside, chrome-spinel, olivine (altered), ilmenite, jeppeite, and priderite. A backscattered electron image showing an hexagonal crystal of haggertyite and associated minerals is shown in Figure 1.

### PHYSICAL AND OPTICAL PROPERTIES

Haggertyite is opaque with a metallic luster. Its crystals occur as thin platelets, occasionally exhibiting an hexagonal morphology. The forms of crystals excavated from thin sections are {001} and {100}. The maximum crystal size observed was about 100  $\mu\text{m}$ . The crystals have ir-

regular to conchoidal fracture. Measurements of  $\text{VHN}_{50}$  using a Leitz Durimet instrument gave values in the range 460 to 540 on three different crystals, with a mean of 500 from five indentations. All of the measurable indentations were perfect but irregularly fractured outward from their corners. The VHN values may be underestimated because they were made on grains in a polished thin section and the depth of the indentations were 10–12  $\mu\text{m}$  compared to the thin section thickness of 30  $\mu\text{m}$ . The hardness of haggertyite is lower than the mean  $\text{VHN}_{100}$  for hawthorneite of 801 (Haggerty et al. 1989) but higher than that reported by Dong et al. (1983) for yimengite,  $\text{VHN}_{25} = 273$ . Approximate Mohs hardness equivalents are haggertyite = 5, hawthorneite = 6, and yimengite = 4.

In plane-polarized reflected light, haggertyite is an undistinguished light gray, similar in reflectance to coexisting priderite (K,Ba)  $(\text{Ti,Fe}^{3+})_8\text{O}_{16}$ . Haggertyite is not noticeably bireflectant; neither is it pleochroic, but between crossed polars some grains are just perceptibly anisotropic, with dark-brown rotation colors or tints. No internal reflections were observed. Three grains of haggertyite in polished thin section were selected for reflectance measurement. Two were sensibly isotropic and the other one was very weakly bireflectant and anisotropic. The specular reflectance values were measured in the visible spectrum from 400 to 700 nm with a Zeiss MPM 800 microscope-spectrophotometer. Measurements were made relative to an SiC reflectance standard (Zeiss, 472), in air

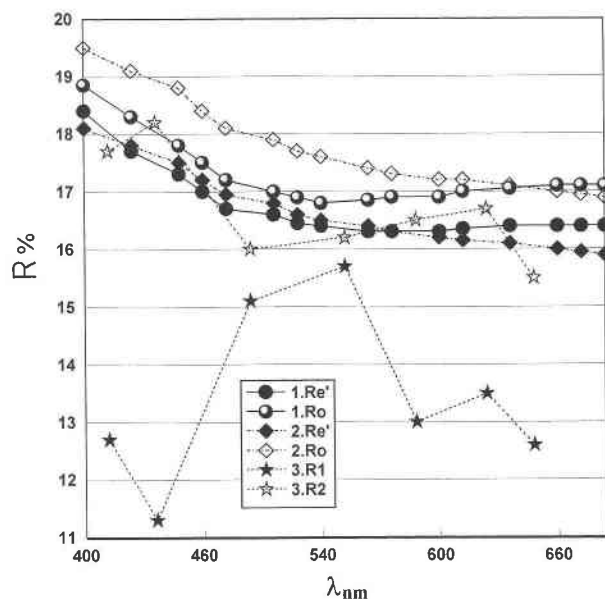


FIGURE 2. Reflectance curves for (1) haggertyite, (2) hawthorneite (Haggerty et al. 1989), and (3) yimengite (Dong et al. 1983), as indicated in the inset.

and in an immersion oil (Zeiss,  $ND = 1.515$ ), with  $\times 50$ , N.A. 0.8, Epiplan Neofluar objectives that were adjusted to provide effective numerical apertures of 0.3. The diameter of the measured area (disc) for each grain was 8  $\mu\text{m}$ . In Table 1<sup>1</sup>, where the values for the bireflectant grain are quoted,  $R_o$  is assigned to the reflectance spectrum from the anisotropic grain that matches those from the isotropic grains.

Reflectance data for haggertyite are presented in Figure 2, which also includes those for hawthorneite (Haggerty et al. 1989), and yimengite (Dong et al. 1983). It is apparent that so far as the visible spectrum is concerned, the only difference between hawthorneite and haggertyite is that the latter is more weakly bireflectant, particularly at the shorter wavelengths. The data for one of the vibration directions for yimengite,  $R_1$ , is similar to those for the other two minerals, but the data for the other reflecting direction,  $R_2$ , are inconsistent with data for haggertyite and hawthorneite. The reflectance spectra were used to derive the optical constants at each wavelength from the Fresnel and Koenigsberger equations (Criddle 1990). The former, assuming the absorption to be zero, gave refractive indices at 590 nm for the air reflectances of 2.35–2.40, and 2.38–2.42 for the oil reflectances. These values are almost certainly too high, given the fact that the mineral is not transparent. On this basis, the refractive indices of 2.30 and 2.33 with corresponding absorption coefficients of 0.33 and 0.34 as calculated using the Koenigs-

TABLE 2. Electron microprobe data for haggertyite\*

Constituent	Mean (wt%)	Range (wt%)	Standard deviation	Atoms per 19 O
TiO <sub>2</sub>	39.1	36.5–41.6	0.8	5.05
FeO†	41.2	39.4–42.9	1.0	3.91 Fe <sup>2+</sup> 2.01 Fe <sup>3+</sup>
MgO	2.7	0.7–3.6	0.5	0.69
MnO	0.80	0.6–1.1	0.08	0.12
NiO	0.25	0.1–0.4	0.06	0.03
Cr <sub>2</sub> O <sub>3</sub>	1.4	0.0–5.6	1.0	0.19
BaO	10.1	9.5–10.5	0.2	0.68
K <sub>2</sub> O	1.42	1.3–1.5	0.04	0.31

\* Average of 56 analyses.

† Total iron reported as FeO. Fe<sup>2+</sup>/Fe<sup>3+</sup> in column 5 calculated to give charge balance.

berger equations, are more realistic. These compare favorably with the mean refractive index calculated using the Gladstone-Dale relations (from the unit-cell composition and calculated density) of 2.30. For the Compatibility Index (Mandarino 1981), the match qualifies as “superior” when absorption is assumed, and “good” when using the values appropriate to zero absorption.

## CHEMICAL COMPOSITION

Wavelength-dispersive electron microprobe data for haggertyite were collected using a Cameca SX-50 instrument, operated at 15 kV and 20 nA. The standards used were MnTiO<sub>3</sub> (TiK $\alpha$ , MnK $\alpha$ ), Fe<sub>2</sub>O<sub>3</sub> (FeK $\alpha$ ), natural diopside (MgK $\alpha$ , SiK $\alpha$ ), NiO (NiK $\alpha$ ), barite (BaLa), orthoclase (KK $\alpha$ ), and Cr<sub>2</sub>O<sub>3</sub> (CrK $\alpha$ ). The range of weight percent values as oxides, their mean values, and their standard deviations from 56 analyses on several crystals from four thin sections are reported in Table 2. Also given in Table 2 are the number of atoms of each metal, normalized to 19 O atoms. Direct chemical analyses for FeO and Fe<sub>2</sub>O<sub>3</sub> could not be performed because of the minute quantity of sample (isolated crystals of typically 30–70  $\mu\text{m}$  in thin sections). The Fe<sup>2+</sup> and Fe<sup>3+</sup> values in Table 2 were calculated to give charge balance according to the magnetoplumbite formula AM<sub>12</sub>O<sub>19</sub>. Within individual crystals, variations on the order of 2–3 wt% occurred for the oxides of Fe, Ti, Cr, and Ba. Increases in Fe, Ti, and K were correlated with decreases in Cr and Ba. Linear regression of a plot of [Fe+Ti] vs. [Cr] gave a slope of  $-1$  ( $R^2 = 0.66$ ), corresponding to the coupled substitution  $\text{Fe}^{2+} + \text{Ti}^{4+} \leftrightarrow 2 \text{Cr}^{3+}$ . The empirical formula calculated from the mean microprobe analyses normalized to 19 O atoms and 12 small cations as in magnetoplumbite is:  $\text{Ba}_{0.68}\text{K}_{0.31}\text{Ti}_{5.05}\text{Fe}_{3.91}^{2+}\text{Fe}_{2.01}^{3+}\text{Mg}_{0.69}(\text{Cr},\text{Mn},\text{Ni})_{0.34}\text{O}_{19}$ . A simplified form of the formula, rounded to whole numbers, is  $\text{Ba}[\text{Ti}_5\text{Fe}_4^{2+}\text{Fe}_2^{3+}\text{Mg}]_{19}\text{O}_{19}$ .

## X-RAY CRYSTALLOGRAPHY

X-ray precession photographs indicated that crystals of haggertyite that were excavated from thin sections were untwinned and gave sharp diffraction patterns. They displayed hexagonal symmetry with approximate cell dimensions  $a = 5.9$  and  $c = 23.3$  Å. The systematic ex-

<sup>1</sup> For a copy of Tables 1 and 6, Document AM-98-017, contact the Business Office of the Mineralogical Society of America (see inside front cover of recent issue) for price information. Deposit items may also be available on the *American Mineralogist* web site at <http://www.minsocam.org>.

**TABLE 3.** Positional and isotropic displacement parameters for haggertyite

Site	Site occupancy*	x	y	z	$U$ (Å <sup>2</sup> )
A	Ba <sub>0.69</sub> K <sub>0.31</sub>	½	¾	¾	0.0136(3)
M(1)	Fe <sub>0.38(4)</sub> Ti <sub>0.56</sub>	0	0	0	0.0109(6)
M(2)	Fe <sub>0.78(5)</sub> Ti <sub>0.12</sub> †	0	0	0.2586(1)	0.0101(7)
M(3)	Fe <sub>0.72(4)</sub> Ti <sub>0.22</sub>	½	¾	0.02658(6)	0.0131(5)
M(4)	Fe <sub>0.32(3)</sub> Ti <sub>0.62</sub>	½	¾	0.19034(6)	0.0115(5)
M(5)	Fe <sub>0.44(2)</sub> Ti <sub>0.50</sub>	0.16780(8)	0.33561(15)	0.89243(3)	0.0113(3)
O(1)	0	0	0	0.1523(3)	0.017(1)
O(2)	½	¾	0.9408(3)	0.014(1)	
O(3)	0.1841(5)	0.3682(10)	¼	0.014(1)	
O(4)	0.1495(3)	0.2989(6)	0.0529(2)	0.012(1)	
O(5)	0.4998(3)	0.9996(6)	0.1504(1)	0.013(1)	

\* 0.06 Mg in sites M(1) to M(5).

† Statistical half occupancy of M(2) site.

**TABLE 4.** Selected interatomic distances (Å) in haggertyite

Metal-oxygen distances		Metal-metal distances†	
A-O(5) (×6)	2.889(4)	A-M(2)	3.433(1)
A-O(3) (×6)	2.973(2)	A-M(4)	3.699(1)
(A-O)	2.931(2.889)*	A-M(5)	3.735(1)
M(1)-O(4) (×6)	1.972(3) (1.968)	M(1)-M(5) e	3.047(1)
M2-O3 (×3)	1.904(5)	M(2)-M(2) (split)	0.400(5)
M2-O1	2.080(7)		
M2-O1'	2.480(7)	M(3)-M(5) c	3.519(2)
(M2-O)tet	1.948(1.967)	M(3)-M(1) c	3.484(2)
M(3)-O(4) (×3)	1.988(4)		
M(3)-O(2)	2.002(6)	M(4)-M(4) f	2.786(3)
(M3)-O)	1.992(1.992)	M(4)-M(5) c	3.542(2)
M(4)-O(5) (×3)	1.948(4)	M(5)-M(5) e	2.948(2)
M(4)-O(3) (×3)	2.072(4)		
(M4)-O)	2.010(1.986)		
M(5)-O(5) (×2)	1.981(2)		
M(5)-O(1)	2.017(4)		
M(5)-O(2)	2.043(4)		
M(5)-O(4) (×2)	2.077(3)		
(M5)-O)	2.029(1.989)		

\* Mean distances in parentheses for hawthorneite (Grey et al. 1987).

† e, c, f refer to edge-, corner- and face-sharing of polyhedra.

tinctions were consistent with space groups  $P6_3/mmc$ ,  $P6_3mc$ , and  $P6_3c$ . The cell dimensions, symmetry, and intensity distribution of (00 $l$ ) reflections were consistent with haggertyite being isostructural with hawthorneite (Haggerty et al. 1989), both possessing the magnetoplumbite structure.

An hexagonal platelet measuring  $0.09 \times 0.06 \times 0.015$  mm was used for the data collection. The crystal used is shown in Figure 1. Initially a data set was collected using a Siemen's AED diffractometer. However, due to the very small crystal size, poor counting statistics resulted and over one-third of the reflections were rejected on a  $4\sigma_{F_o}$  basis. The data were then re-collected on a Nonius Kappa CCD diffractometer. MoK $\alpha$  radiation was employed at 50 kV and 40 mA. The crystal-to-detector distance was 25 mm. Unit-cell dimensions were refined from data collected on 70 frames obtained by rotating around  $\phi$  in 1° steps,  $a = 5.9369(1)$  Å,  $c = 23.3445(6)$  Å. A full sphere of data was collected out to  $2\theta = 52^\circ$  by rotating  $360^\circ$  around  $\phi$ . Two images were collected at each 1°  $\phi$  interval with a counting time of 70 s per image. A total of 11636 partial reflections were collected that were processed to give 387 unique reflections, with an  $R_{int}$  (on  $I$ ) of 0.058 and a refined mosaicity of 0.455(2). Of the 387 reflections, 339 were considered observed, with  $F_o > 4\sigma_{F_o}$ . Application of an analytical absorption correction, based on indexing of the crystal faces (Sheldrick 1976), gave minimum and maximum transmission factors of 0.51 and 0.78, respectively ( $\mu = 11.2$  mm<sup>-1</sup>).

A satisfactory refinement of the data was made on the basis that haggertyite had a magnetoplumbite-type structure. The refined coordinates for hawthorneite (Grey et al. 1987) in space group  $P6_3/mmc$  were used as starting values, and published data on site occupancies in hawthorneite and other magnetoplumbite-type structures were used to make initial cation site assignments. The expected ordering of magnesium (with ferrous iron) in the tetrahedral site M(3) of the spinel block gave a relatively high residual,  $R_1 = 0.063$  and a low isotropic displacement parameter for M(3). From different refinements it was found that the best fit to the data was obtained with a

statistical distribution of the magnesium over the five M atom sites. In the final refinement the Fe/Ti occupancies at each of the M sites were released. Refinement on  $F^2$  of 30 coordinates, site occupancies, and isotropic displacement parameters converged at  $R_1 = 0.037$  and  $wR_2 = 0.09$  for all data and  $R_1 = 0.034$  for the 339 reflections with  $F_o > 4\sigma_{F_o}$ . A difference Fourier map showed no unusual features. The largest peak,  $0.6$  e/Å<sup>3</sup>, was  $1.1$  Å from O(2). The refinements were made using SHELX-93 (Sheldrick 1993). Final coordinates and isotropic displacement parameters are given in Table 3. Polyhedral bond lengths and angles are reported in Table 4. The minute quantity of tiny crystals of haggertyite limited the quality of the powder pattern for the mineral. Instead, the refined structural parameters were used in the Rietveld program SR5 (Hill and Howard 1986) to generate a calculated powder pattern for haggertyite, and this is presented in Table 5. The observed and calculated structure factors are presented in Table 6<sup>1</sup>.

## DISCUSSION

### Description of the structure

Haggertyite is isostructural with the magnetoplumbite-type phases hawthorneite and yimengite. A polyhedral representation of the structure, with atom labeling, is shown in Figure 3. It is based on a closest-packed anion framework with small cations distributed over five independent octahedral and tetrahedral sites. The anion layers are parallel to (001), and have a mixed-layer stacking sequence given by (cchh'hcchh'h...) where  $c$  and  $h$  symbolize cubic and hexagonal stacking. The  $h'$  layers have one quarter of the O atoms substituted by the large A cations (Ba and K), giving layers of composition  $AO_3$ .

The magnetoplumbite structure is commonly described in terms of intergrowth of (001) slabs of R-blocks and S-blocks (Obador et al. 1985), according to the scheme RSR\*S\*. . . The \* symbol indicates that the block has

**TABLE 5.** Calculated X-ray powder diffraction data for haggertyite

$d_{\text{calc}}$	$hkl$	$l/l_0$	$d_{\text{calc}}$	$hkl$	$l/l_0^*$
5.012	0 1 1	4	2.141	0 2 6	24
4.697	0 1 2	10	1.959	0 1 11	5
3.887	0 0 6	10	1.933	1 2 1	1
3.852	0 1 4	2	1.832	1 1 10	2
3.098	0 1 6	2	1.823	0 2 9	7
2.963	1 1 0	44	1.726	0 2 10	4
2.915	0 0 8	11	1.711	0 3 0	7
2.872	1 1 2	6	1.693	0 3 2	2
2.795	0 1 7	90	1.676	1 2 7	37
2.641	1 1 4	100	1.666	0 0 14	6
2.566	0 2 0	9	1.641	1 3 4	20
2.551	0 2 1	6	1.634	10 2 11	47
2.535	0 1 8	7	1.625	1 1 12	3
2.506	0 2 2	3	1.615	1 2 8	6
2.437	0 2 3	46	1.549	0 2 12	4
2.356	1 1 6	3	1.481	2 2 0	47
2.248	0 2 5	30			

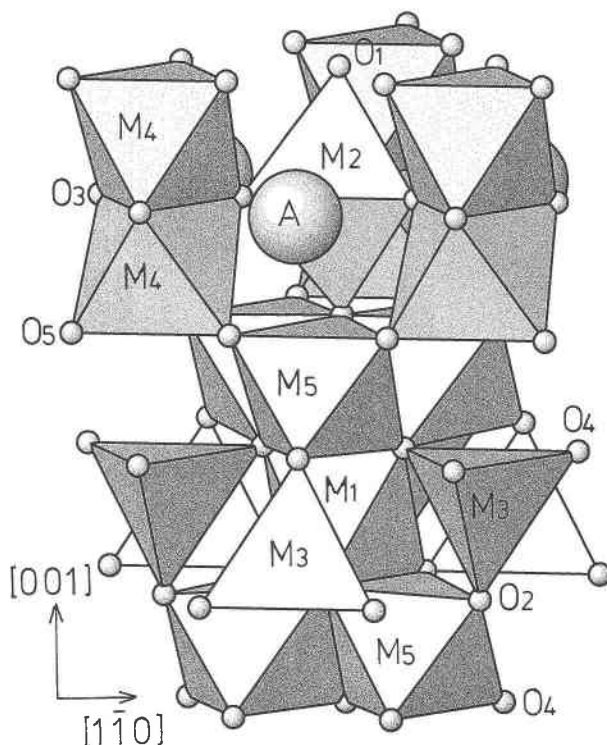
\* Intensities &lt;1 not shown.

been rotated 180° about  $c$  relative to the preceding block. The stacking of the two types of blocks is illustrated in Figure 4. The S-block has the well-known spinel structure. It comprises two cubic-stacked O atom layers [ $\equiv(111)_{\text{sp}}$  layers] and three metal atom layers, with composition  $M(1)M(3)_2M(5)_{6/2}O_8 \equiv M_6O_8$  (The 6/2 means the 6 M(5) atoms are shared with the R-block). M(1) and M(5) are octahedrally coordinated and M(3) is tetrahedrally coordinated.

The R-block involves three hexagonal-stacked anion layers and has the composition  $AM(2)M(4)_2M(5)_{6/2}O_{11} \equiv AM_6O_{11}$ . The R-block is a common structure element in many hexagonal barium ferrites and exists independently in  $BaFe_4Ti_2O_{11}$  (Obradors et al. 1983). In the R-block, M(4) and M(5) are octahedrally coordinated. Pairs of M(4) octahedra share a common face in the  $BaO_3$  layers that lie on mirror planes at  $z = \pm 1/4$ . The  $BaO_3$  layer with the associated pairs of face-shared octahedra,  $M(4)_2O_9$ , represents an element of hexagonal  $BaTiO_3$  (Burbank and Evans 1948).

The M(2) cations in the R-block are statistically distributed, with 50% occupancy, over pairs of tetrahedral sites that share a common face in the mirror plane. If M(2) occupied the site (0, 0, 1/4) in the mirror plane it would have trigonal bipyramidal coordination to five O atoms. However, numerous structure refinements for magnetoplumbite-type phases have shown that the M(2) cations are displaced from the mirror plane along [001] by typically 0.1 to 0.2 Å into the adjacent tetrahedral sites, giving 4 + 1 coordination (Graetsch and Gebert 1996). In haggertyite, M(2) is displaced 0.200(3) Å from the mirror plane, which is significantly greater than in hawthorneite, 0.164(7) Å (Grey et al. 1987). This displacement gives three basal M(2)-O(3) distances of 1.904(5) Å, and an apical M(2)-O(1) distance of 2.080(7), plus a fifth coordinated O atom at a longer M(2)-O(1) distance of 2.480(7) Å.

The nature (dynamical or static disorder) and energetic

**FIGURE 3.** Polyhedral representation of the structure of haggertyite, viewed approximately along [110]. Selected sites are labeled.

origin of the displaced M(2) atom has been the subject of much conjecture in the literature. Mossbauer data for  $BaFe_{12}O_{19}$  has been interpreted in terms of dynamical disorder, at least at temperatures above 75 K (Kreber et al. 1975; Obradors et al. 1985). Electrostatic factors favor an undisplaced M(2) atom with trigonal bipyramidal coordination. Graetsch and Gebert (1996) have proposed that this is prevented by electronic repulsion between M(2) and the basal-plane O(3) O atoms. Another possible contributing factor is the role of metal-metal non-bonded repulsions, particularly those involving the large A atoms for which closed-shell electronic repulsions can be important. From Table 4, the shortest metal-metal distance involving the A atom is to M(2). The A-M(2) distance of 3.433(2) Å is shorter than in BaM alloys such as BaZn (Ba-Zn = 3.54 Å). Displacement of M(2) along [001] increases its separation from A, and at the same time it increases the shielding of electrostatic forces between A and M(2) by the intervening O atoms. Non-bonding metal-metal repulsions also appear to play a role in the S-block. Valence sum calculations for S-block metal atom sites in magnetoplumbite structures show that the octahedral site M(1) is oversaturated and the tetrahedral site M(3) is undersaturated (e.g., see Table IV in Obradors et al. 1985). The effect is more pronounced in aluminates than in ferrites. Wagner and O'Keeffe (1988) have attributed long tetrahedral Al-O bond lengths in the S-blocks

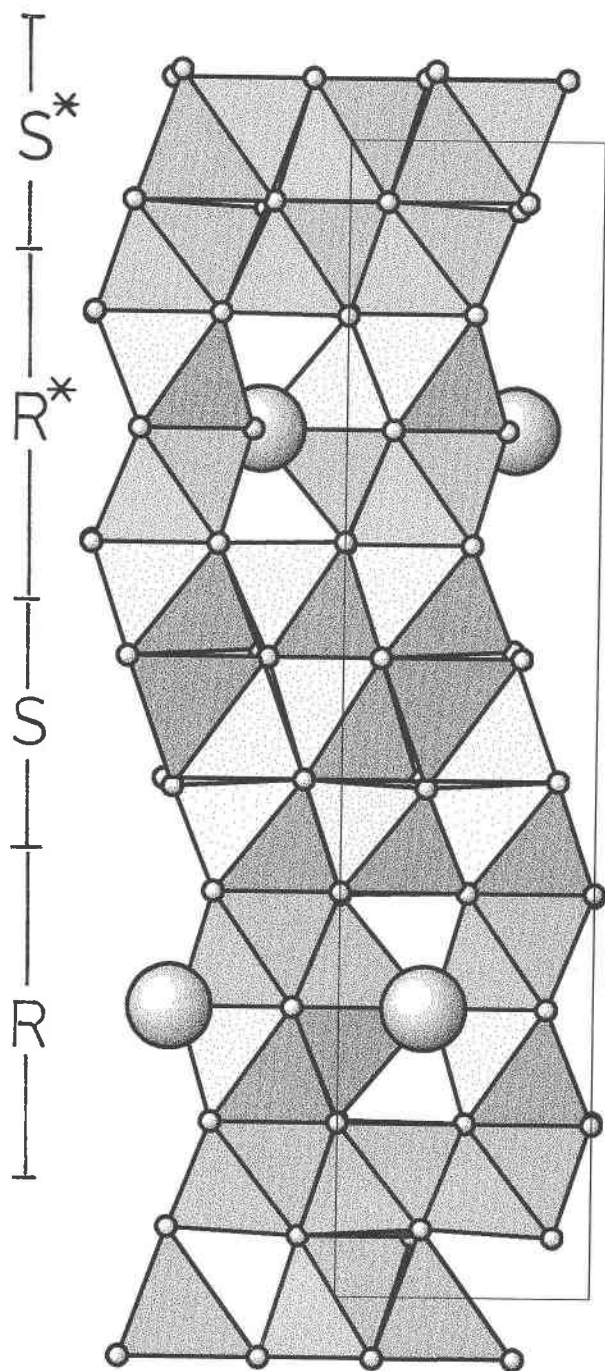


FIGURE 4. Stacking of S-blocks and R-blocks in haggertyite, viewed in projection along [100]. Unit-cell outline shown, as light lines,  $c$  axis is perpendicular to the page.

of  $\beta$ -aluminas and magnetoplumbites to non-bonded Al-Al repulsions.

The calculated number of titanium atoms per formula unit (apfu) from the refined site occupancies (Table 3) is 5.4, which is in reasonable agreement with the value of 5.0 Ti apfu obtained by microprobe analysis. The refine-

ment results show that the tetrahedral sites M(2) and M(3) are enriched in Fe whereas the octahedral sites M(1) and M(4) are slightly enriched in Ti. Equivalent cation distributions were obtained in a refinement of the  $\text{Co}^{2+}$ -containing magnetoplumbite-type phase  $\text{SrTi}_6\text{Co}_6\text{O}_{19}$  (Graetsch and Gebert 1995). Their calculations of the Madelung part of the lattice energy showed that ordering of the tetravalent cation in the face-shared octahedral site M(4) and of the divalent cation in the tetrahedral site M(3) are electrostatically favored. Comparison of the average bond lengths for the different metal atom sites in haggertyite with those for hawthorneite (given in parentheses in Table 4) suggests that  $\text{Fe}^{2+}$  is predominantly ordered in the tetrahedral site M(3) and the octahedral site M(4). A more quantitative evaluation of cation ordering using valence sum calculations is not warranted because the many species ( $\text{Fe}^{2+}$ ,  $\text{Fe}^{3+}$ , Ti, and Mg) allows many possible solutions. The mixing of cations having significantly different sizes and valence states at the metal atom sites in haggertyite is reflected in large atomic displacement parameters shown in Table 3. Graetsch and Gebert (1995) noted similar elevated atomic displacement parameters in  $\text{SrTi}_6\text{Co}_6\text{O}_{19}$ , compared to those in magnetoplumbite-type compounds containing only trivalent small cations.

#### Related minerals and paragenesis

The compositional distinctions between the minerals haggertyite, hawthorneite, and yimingite are readily seen by comparing their simplified formulae; haggertyite,  $\text{Ba}[\text{Ti}_3\text{Fe}_2^{2+}\text{Fe}_2^{3+}\text{Mg}]_{19}\text{O}_{19}$ , hawthorneite,  $\text{Ba}[\text{Ti}_3\text{Cr}_4\text{Fe}_2^{2+}\text{Fe}_2^{3+}\text{Mg}]_{19}\text{O}_{19}$ , and yimingite,  $\text{K}[\text{Ti}_3\text{Cr}_3\text{Fe}_2^{3+}\text{Mg}_2]_{19}\text{O}_{19}$ . The latter two minerals are clearly distinguished on the basis of having different A cations. The decrease in valency of the A cation from  $\text{Ba}^{2+}$  in hawthorneite to  $\text{K}^+$  in yimingite is balanced by a coupled replacement of  $\text{M}^{2+}$  ( $\text{M} = \text{Mg}, \text{Fe}$ ) by  $\text{Cr}^{3+}$ . Haggertyite has the same dominant A cation as hawthorneite, but differs in the replacement of  $2\text{Cr}_2\text{O}_3$  by  $2\text{FeTiO}_3$ . In hawthorneite the Cr is ordered in the octahedral sites M(1) and M(5) (Grey et al. 1987) whereas in haggertyite these sites are occupied by predominantly Fe + Ti. The justification for the two different mineral names is based on the different dominant cations in these crystallographic sites. The substitution  $2\text{Cr}^{3+} \leftrightarrow \text{Fe}^{2+} + \text{Ti}^{4+}$  is reflected in the relatively large (3.5%) increase in cell volume from hawthorneite to haggertyite. It also is reflected in compositional zoning in individual haggertyite crystals as detected by electron microprobe analyses, with chromium contents decreasing toward the rims of crystals. The chromium content of both haggertyite and priderite is low, despite the close association with chrome-spinel, and this indicates metasomatic conditions different to those that gave rise to the hawthorneite-bearing xenoliths (Haggerty et al. 1989) in kimberlite pipes in South Africa or to yimingite from kimberlitic rocks in Venezuela (Nixon and Condliffe 1989).

Haggertyite was found exclusively within the reaction zones separating mafic xenoliths and the lamproite proper.

In comparison with the lamproite the xenoliths are Si- and Fe-rich, and it is considered that these elements were supplied to the reaction zone, while Ba and Ti were derived from the lamproite. A distinct feature of the reaction zones is that they contain no perovskite, although this is an ubiquitous accessory mineral in the lamproite. Decomposition of perovskite (in the presence of silica) could provide the Ti source for haggertyite, with the Ca reacting to form diopside, which commonly rings the xenolith core (as described also by Mitchell and Lewis 1983). Cr-spinel and haggertyite are commonly found in close spatial association in the reaction zones (e.g., Fig. 1). In one instance a small (<10  $\mu\text{m}$ ) rounded low-Cr spinel (~20 wt%  $\text{Cr}_2\text{O}_3$ ) grain was found within haggertyite, consistent with a reaction similar to that of Haggerty et al. (1989). It is not certain if this reaction mechanism can be extended to all subhedral homogeneous haggertyite crystals. A study of the mineralogy and paragenesis of the xenolith reaction zones in the Prairie Creek lamproite is currently being undertaken and a more detailed presentation will be separately reported (Velde, in preparation).

#### ACKNOWLEDGMENTS

We thank Leo Straver of Nonius N.V., Delft, for help with the single crystal data intensity collection. We appreciate the efforts of Joseph D. Ferrara and colleagues at Molecular Structure Corporation, Houston, Texas, who collected an independent intensity data set on haggertyite using a Rigaku CCD diffractometer and confirmed the structure refinement reported here. We thank P. Blanc, H. Remy, M. Fialin, and C. Richard of the University of Paris 6 for help with the scanning electron microscopy and electron microprobe studies.

#### REFERENCES CITED

- Adelskold, V. (1938) X-ray studies on magneto-plumbite,  $\text{PbO} \cdot 6\text{Fe}_2\text{O}_3$ , and other substances resembling "beta-alumina",  $\text{Na}_2\text{O} \cdot 11\text{Al}_2\text{O}_3$ , *Arkiv for Kemi Mineralogisch Geologi*, Series A-12, 29, 1-9.
- Burbank, R.D. and Evans, H.T. Jr. (1948) The crystal structure of hexagonal barium titanate. *Acta Crystallographica*, 1, 330-336.
- Criddle, A.J. (1990) The reflected-light polarizing microscope and microscope-spectrophotometer. In: J.L. Jambor and D.J. Vaughan, Eds., *Advanced Microscopic Studies of Ore minerals*. Short Course Handbook 17, p. 1-36. Mineralogical Association of Canada, Ottawa.
- Dong, Z., Zhou, J., Lu, Q., and Peng, Z. (1983) Yimengite (K)(Cr, Ti, Fe, Mg) $_2\text{O}_{19}$ —A new mineral. *Kexue Tongbao Bulletin Science*, 15, 932-936.
- Graetsch, H. and Gebert, W. (1995) Cation distribution in magnetoplumbite type  $\text{SrTi}_2\text{Co}_6\text{O}_{19}$ . *Zeitschrift für Kristallographie*, 210, 9-13.
- (1996) Short  $\text{Cr}^{3+}$ - $\text{Cr}^{3+}$  distances in magnetoplumbite type  $\text{SrCr}_2\text{Ga}_4\text{O}_{19}$ . *Zeitschrift für Kristallographie*, 211, 25-30.
- Grey, I.E., Madsen, I.C., and Haggerty, S.E. (1987) Structure of a new upper-mantle, magnetoplumbite-type phase,  $\text{Ba}[\text{Ti}_2\text{Cr}_2\text{Fe}_4\text{Mg}]\text{O}_{19}$ . *American Mineralogist*, 72, 633-636.
- Haggerty, S.E., Erlank, A.J., and Grey, I.E. (1986) Metasomatic mineral titanate complexing in the upper mantle. *Nature*, 319, no. 6056, 761-763.
- Haggerty, S.E., Grey, I.E., Madsen, I.C., Criddle, A.J., Stanley, C.J., and Erlank, A.J. (1989) Hawthorneite,  $\text{Ba}[\text{Ti}_2\text{Cr}_2\text{Fe}_4\text{Mg}]\text{O}_{19}$ : A new metasomatic magnetoplumbite-type mineral from the upper mantle. *American Mineralogist*, 74, 668-675.
- Hill, R.J. and Howard, C.J. (1986). A computer program for Rietveld analysis of fixed-wavelength X-ray and neutron powder diffraction patterns. Australian Atomic Energy Commission Report M112.
- Kreber, E., Gonser, U., Trautwein, A., and Harris, F.E. (1975). Mossbauer measurements of the bipyramidal site in  $\text{BaFe}_{12}\text{O}_{19}$ . *Journal of Physics and Chemistry of Solids*, 36, 263-265.
- Mandarino, J.A. (1981) The Gladstone-Dale relationship. IV. The compatibility concept and its application. *Canadian Mineralogist*, 19, 441-450.
- Mitchell, R.H. (1985) A review of the mineralogy of lamproites. *Transactions of the Geological Society of South Africa*, 88, 411-437.
- Mitchell, R.H. and Lewis, R.D. (1983) Priderite-bearing xenoliths from the Prairie Creek mica peridotite, Arkansas. *Canadian Mineralogist*, 21, 59-64.
- Mullen, E.D. and Murphy, S.G. (1985) Petrology of the Arkansas alkalic province: a summary of previous and new investigations. A guidebook for GSA regional meeting, Fayetteville, Arkansas. April 16-18, p. 34-62.
- Nixon, P.H. and Condliffe, E. (1989) Yimengite of K-Ti metasomatic origin in kimberlitic rocks from Venezuela. *Mineralogical Magazine*, 53, 305-309.
- Obradors, X., Collomb, A., Pannetier, J., Isalgue, A., Tejada, J., and Joubert, J.C. (1983) Crystal Structure and cationic distribution of  $\text{BaFe}_2\text{Ti}_2\text{O}_{11}$  R-type hexagonal ferrite. *Materials Research Bulletin*, 18, 1543-1553.
- Obradors, X., Collomb, A., Pernet, M., Samaras, D., and Joubert, J.C. (1985) X-ray analysis of the structural and dynamic properties of  $\text{BaFe}_2\text{Ti}_2\text{O}_{11}$  hexagonal ferrite at room temperature. *Journal of Solid State Chemistry*, 56, 171-181.
- Sheldrick, G.M. (1976) SHELX 76, Program for Crystal Structure Determination, University of Cambridge, Cambridge, U.K.
- (1993) SHELXL93, Program for the Refinement of Crystal Structures, University of Göttingen, Germany.
- Wagner, T.R. and O'Keeffe, M. (1988) Bond lengths and valences in aluminates with the magnetoplumbite and  $\beta$ -alumina structures. *Journal of Solid State Chemistry*, 73, 211-216.

MANUSCRIPT RECEIVED NOVEMBER 24, 1997

MANUSCRIPT ACCEPTED JULY 16, 1998

PAPER HANDLED BY LEE A. GROAT